Ppb-level detection of nitric oxide using an external cavity quantum cascade laser based QEPAS sensor

Lei Dong,[1,*] Vincenzo Spagnolo,[1,2] Rafał Lewicki,[1] and Frank K. Tittel[1]

[1]*Department of Electrical and Computer Engineering, Rice University, 6100 Main Street, Houston, TX 77005, USA*
[2]*Dipartimento Interateneo di Fisica,University and Politecnico of Bari, CNR-IFN UOS BARI,Via Amendola 173, 70126 Bari, Italy*
[*]*lei.dong@rice.edu*

Abstract: Geometrical parameters of micro-resonator for a quartz enhanced photoacoustic spectroscopy sensor are optimized to perform sensitive and background-free spectroscopic measurements using mid-IR quantum cascade laser (QCL) excitation sources. Such an optimized configuration is applied to nitric oxide (NO) detection at 1900.08 cm^{-1} (5.26 μm) with a widely tunable, mode-hop-free external cavity QCL. For a selected NO absorption line that is free from H_2O and CO_2 interference, a NO detection sensitivity of 4.9 parts per billion by volume is achieved with a 1-s averaging time and 66 mW optical excitation power. This NO detection limit is determined at an optimal gas pressure of 210 Torr and 2.5% of water vapor concentration. Water is added to the analyzed mixture in order to improve the NO vibrational-translational relaxation process.

OCIS codes: (280.3420) Laser sensors; (140.3070) Infrared and far-infrared lasers; (300.6390) Spectroscopy, molecular.

References and links

1. J. H. Seinfeld and S. N. Pandis, *Atmospheric Chemistry and Physics: from Air Pollution to Climate Change* (Wiley, New York, 1998).
2. M. R. McCurdy, A. Sharafkhaneh, H. Abdel-Monem, J. Rojo, and F. K. Tittel, "Exhaled nitric oxide parameters and functional capacity in chronic obstructive pulmonary disease," J Breath Res **5**(1), 016003 (2011).
3. T. H. Risby, "Current status of mid-infrared quantum and interband cascade lasers for clinical breath analysis," Opt. Eng. **49**(11), 111123 (2010).
4. A. A. Kosterev, Y. A. Bakhirkin, R. F. Curl, and F. K. Tittel, "Quartz-enhanced photoacoustic spectroscopy," Opt. Lett. **27**(21), 1902–1904 (2002).
5. R. Lewicki, G. Wysocki, A. A. Kosterev, and F. K. Tittel, "Carbon dioxide and ammonia detection using 2μm diode laser based quartz-enhanced photoacoustic spectroscopy," Appl. Phys. B **87**(1), 157–162 (2007).
6. L. Dong, A. A. Kosterev, D. Thomazy, and F. K. Tittel, "QEPAS spectrophones: design, optimization, and performance," Appl. Phys. B **100**(3), 627–635 (2010).
7. L. Dong, A. A. Kosterev, D. Thomazy, and F. K. Tittel, "Compact portable QEPAS multi-gas sensor," Proc. SPIE **7945**, 50Q–1 (2011).
8. A. A. Kosterev, L. Dong, D. Thomazy, F. K. Tittel, and S. Overby, "QEPAS for chemical analysis of multi-component gas mixtures," Appl. Phys. B **101**(3), 649–659 (2010).
9. V. Spagnolo, A. A. Kosterev, L. Dong, R. Lewicki, and F. K. Tittel, "NO trace gas sensor based on quartz enhanced photoacoustic spectroscopy and external cavity quantum cascade laser," Appl. Phys. B **100**(1), 125–130 (2010).
10. C. Bauer, U. Willer, and W. Schade, "Use of quantum cascade laser for detection of explosives: progress and challenges," Opt. Eng. **49**(11), 111126 (2010).
11. L. S. Rothman, A. Barbe, C. D. Brenner, L. R. Brown, C. Camy-Peyret, M. R. Carleer, K. Chance, C. Clerbaux, V. Dana, V. M. Devi, A. Fayt, J. M. Flaudi, R. R. Gamache, A. Goldman, D. Jacquemart, K. W. Jucks, W. J. Lafferty, J. Y. Mandin, S. T. Massie, V. Nemtchinov, D. A. Newnham, A. Perrin, C. P. Rinsland, J. Schroeder, K. M. Smith, M. A. H. Smith, K. Tang, R. A. Toth, J. Vander Auwera, P. Varanasi, and K. Yoshino, "The HITRAN Molecular Spectroscopic Database: Edition of 2000 including updates through 2001," J. Quant. Spectrosc. Radiat. Transf. **82**(1-4), 5–44 (2003).
12. T. L. Cottrell and J. C. McCoubrey, *Molecular Energy Transfer In Gases* (Butterworths, London, 1961).

#153576 - $15.00 USD Received 7 Sep 2011; revised 22 Oct 2011; accepted 27 Oct 2011; published 10 Nov 2011

13. R. D. Grober, J. Acimovic, J. Schuck, D. Hessman, P. J. Kindlemann, J. Hespanha, A. S. Morse, "Fundamental limits to force detection using quartz tuning forks," Rev. Sci. Instrum. **71**(7), 2776–2780 (2000).
14. A. A. Kosterev, F. K. Tittel, D. V. Serebryakov, A. L. Malinovsky, and I. V. Morozov, "Applications of quartz tuning forks in spectroscopic gas sensing," Rev. Sci. Instrum. **76**(4), 043105 (2005).
15. S. Gray, A. Liu, F. Xie, and C. E. Zah, "Detection of nitric oxide in air with a 5.2 μm distributed-feedback quantum cascade laser using quartz-enhanced photoacoustic spectroscopy," Opt. Express **18**(22), 23353–23357 (2010).
16. R. Sarmiento, I. E. Santosa, S. T. Persijn, L. J. J. Laarhoven, and F. J. M. Harren, "Trace nitric oxide detection using CO-laser photoacoustic spectroscopy," *in Proceedings Forum Acusticum 2005*, p.L139, Budapest (2005).
17. A. A. Kosterev, Y. A. Bakhirkin, F. K. Tittel, S. Mcwhorter, and B. Ashcraft, "QEPAS methane sensor performance for humidified gases," Appl. Phys. B **92**(1), 103–109 (2008).

1. Introduction

The capability of detecting and quantifying nitric oxide (NO) at ppbV concentration levels has an important impact in diverse fields of applications including environmental monitoring, industrial process control and medical diagnostics. The major sources of NO emission into the atmosphere are associated with industrial combustion processes as well as automobile, truck, aircraft and marine transport emissions. Long term, continuous, reliable NO concentration measurements in ambient air are important because of NO's role in the depletion of earth's ozone layer and in the formation of acid rains and smog [1]. Furthermore, it was found that NO is associated with numerous physiological processes in the human body. In particular, NO can be used as a biomarker of asthma and inflammatory lung diseases such as chronic obstructive pulmonary disease [2]. This paper describes development of sensitive and selective sensor technology, capable of detecting and monitoring single ppbV NO concentration levels with a time response of <1 sec, for environmental monitoring and noninvasive exhaled breath analysis [3].

Quartz-enhanced photoacoustic spectroscopy (QEPAS), first reported in 2002, is a gas-sensing technique that features an absorption detection module (ADM) with dimensions of 10-20 mm [4]. QEPAS allows performing sensitive measurement of trace gases in gas sample of a few mm^3 in volume. The QEPAS technique employs a quartz tuning fork (QTF) as a sharply resonant acoustic transducer, instead of a broadband electric microphone used in conventional photoacoustic spectroscopy (PAS). The QTF is a piezo-electric element, capable of detecting weak acoustic waves generated when the modulated optical radiation interacts with a trace gas, and converts the QTF deformation into separation of electrical charges.

In order to further enhance the QEPAS signal, a so-called micro-resonator (mR) can be added to the QTF sensor architecture. The mR typically consists of two metallic [4] or glass tubes [5]. The QTF is positioned between the tubes to probe the acoustic waves excited in the gas contained inside the mR. To date, such a configuration has been used in most reported QEPAS based gas sensors [5–10]. Moreover, a recent optimization study revealed that for a 32kHz QTF, two 4.4 mm-long tubes with 0.5-0.6 mm inner diameter yields the highest QEPAS signal-to-noise ratio (SNR) [6]. These optimum tube parameters have been adopted in a near-infrared (NIR) fiber-coupled semiconductor diode laser based QEPAS sensors where the typical size of the NIR beam spot, after using a fiber-coupled optical focuser, is <100 μm. In such systems, a clear NIR beam passage through the ADM is observed, resulting in zero background and excellent detection results [7, 8]. However, these optimum mR tube parameters are not suitable for a free space mid-infrared (MIR) QEPAS sensor configuration due to much more challenging process of focusing a typical ~3 mm-diameter MIR beam through the mR and 300 μm gap between QTF's prongs. In fact, the radiation blocked by the mR or QTF results in an undesirable non-zero background when absorbed by the ADM structural elements. This background is usually several times larger than the thermal noise level of QEPAS and carries a shifting fringe-like interference pattern, which limits the detection sensitivity of QEPAS [9].

For a typical QCL beam, short mR tubes with a larger inner diameter are advantageous in facilitating optical alignment of the QCL excitation beam with the mR and the QTF. In this

#153576 - $15.00 USD Received 7 Sep 2011; revised 22 Oct 2011; accepted 27 Oct 2011; published 10 Nov 2011

paper, we particularly address this issue by performing experimental measurements using ADMs with different tube sizes so that we were able to determine the optimized geometrical mR parameters to meet a specific QCL based QEPAS application. Subsequently, the optimized mR tubes were applied to the NO detection, using a 5.26 μm, CW, thermoelectrically cooled (TEC), external cavity quantum cascade laser (EC-QCL) commercially available from Daylight Solutions, Inc as an excitation source. We also investigated the effect of different concentrations levels of water vapor in a NO mixture on QEPAS signals, since the concentrations of water vapor may vary from 0 to 5% depending on the specific application. The effective overall characteristic performance of EC-QCL based NO QEPAS sensor was determined.

2. Optimization of QEPAS mR for QCL based sensor applications

To assess the optimum mR performance, the QEPAS SNR must be used as the selection criterion. The amplitude of QEPAS signal is determined by the following five factors: 1. QTF Q factor, 2. enhancement factor of the acoustic mR, 3. peak intensity of the absorption line of the desired trace gas species, 4. vibrational-translational (V-T) relaxation rate of target gas and 5. laser modulation depth. The first four factors depend on pressure, while the fifth factor, the laser modulation depth, must match the pressure dependent absorption line width. In order for the enhancement factor of mR to dominate the amplitude of QEPAS signal, an experimental characterization similar to the one reported in Ref [6] was performed. A C_2H_2 absorption line at 6529.17 cm^{-1} with 6.31×10^{-7} cm^{-1} peak absorption was used as the target line [11]. The C_2H_2 has a fast V-T relaxation rate, 72.8 ns at 25 °C [12], which can be considered instantaneous for the $1/f_0$ time scale where f_0 is the resonant frequency of the QTF. The laser modulation depth was set to the optimal value based on different pressures. Thus, at a certain pressure, the influence of factors 3 to 5 on the amplitude of QEPAS signal can be neglected. Since the interaction of sound wave fields in the mR and between the prongs of QTF impacts the QTF's parameters, the QTF's Q factor is not an independent variable. Hence, the factors 1 to 2 can be combined as one factor, which is determined by the geometrical mR parameters.

It has been verified from theoretical and experimental analysis that the primary noise source affecting measured QEPAS signals is the thermal noise associated with the QTF at the resonant frequency f_0. Its root mean square (rms) voltage noise can be expressed as [13]:

$$\sqrt{V_{rms}^2} = R_g \sqrt{\frac{4k_B T}{R}} \sqrt{\Delta f}, \tag{1}$$

$$R = \frac{1}{Q}\sqrt{\frac{L}{C}}, \tag{2}$$

where Δf is the detection bandwidth, k_B is the Boltzmann constant, T is QTF temperature, R_g is the value of the feedback resistor in transimpedance amplifier, and R, L, and C are the electrical parameters of the QTF when it is represented by the equivalent serial resonant circuit.

The results of SNR as a function of pressure measurements obtained for mR tubes of different lengths and internal diameter size are plotted in Fig. 1. The results of a bare QTF and a QTF with the NIR optimal mR tubes (4.4 mm-long, 0.6 mm inner diameter) are also shown in Fig. 1 as SNR level references. The SNR of the 3.9 mm-long mR tubes are lower but close to that of the NIR optimal length mR tubes, especially at lower pressures. For the pressure ranges between 20 to 100 Torr, the 3.9 mm-long mR tubes with inner diameters of 0.76mm and 0.84mm have practically the same SNR as the NIR optimal mR tubes. In the pressure range between 100 to 250 Torr, the 3.9 mm-long mR tubes with 0.76mm inner diameter

#153576 - $15.00 USD Received 7 Sep 2011; revised 22 Oct 2011; accepted 27 Oct 2011; published 10 Nov 2011

results in the same SNR as the NIR optimal mR tubes, while the 0.84 inner diameter tubes have a ~10% lower SNR. For pressures above 250 Torr, the 3.9 mm-long mR tubes with 0.76

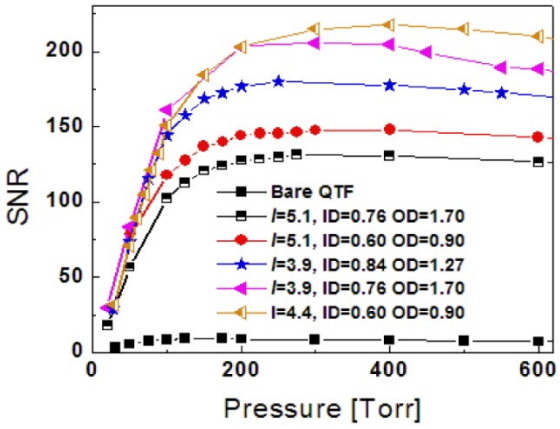

Fig. 1. Signal-to-noise ratio as a function of pressure for mR tubes.of different inner and out diameters; l-length of each mR tube; ID, OD-inner and outer diameter of the mR tube. The data for a bare QTF are shown as a reference.

mm inner diameter result in a 10% decrease of the SNR compared to the SNR for NIR optimal mR tubes. For the 0.84 mm inner diameter tubes, the decrease of the SNR can be up to 20% SNR. When determining the optimum MIR mR parameters, a major design rule is that tubes with wider inner diameter are preferable provided that the SNR does not decrease significantly. Therefore, based on the sensor operating pressure, the geometrical mR parameters can be optimized to achieve MIR SNR values that are close to NIR optimal mR tubes. Table 1 lists the optimal mR tube parameters selection for a QCL based QEPAS sensor for different pressure conditions.

Table 1. Optimal parameters of mR tubes for QCL based QEPAS sensor at different pressures

	l = 3.9 mm	
Pressure, torr	ID = 0.76	ID = 0.84
20-100		Selected
100-250	Selected	Selected
>250	Selected	

3. Experimental setup and optimization of NO QEPAS detection

A schematic of the QEPAS sensor for NO detection is depicted in Fig. 2. The sensor platform is based on a 2*f* wavelength-modulation spectroscopy (WMS) based QEPAS-detection approach. A widely tunable CW EC-QCL (Daylight Solutions, Inc., model 21052-MHF) served as the excitation source for generating the QEPAS signal. The EC-QCL frequency tuning was achieved by applying a voltage to the piezoelectric translator that controls a diffraction grating angle. A continuous spectral tuning range from 1763 to 1949 cm^{-1} was obtained at a QCL operating temperature of 16.5 °C and a maximum QCL current of 450 mA. The diameter of collimated EC-QCL output beam was ~3 mm. Two 25 mm focal length plano-convex Ge lenses with broadband antireflection (AR) coating were used to focus the laser radiation through the mR and the prongs of QTF and to re-collimate the laser beam upon exiting the ADM. A beam diameter of ~20 μm at the center of the prongs of QTF was obtained from a theoretical calculation using the above-mentioned two lenses. Since previous results showed that the optimal pressure range for NO detection is from 150 and 250 Torr [9],

#153576 - $15.00 USD Received 7 Sep 2011; revised 22 Oct 2011; accepted 27 Oct 2011; published 10 Nov 2011

an acoustic mR consisting of two hypodermic tubes, each 3.9 mm long with 0.84 mm inner diameter, was mounted on both side of the QTF based on the results summarized in Table 1. These mR tube parameters result in an optical power transmission of 99% through the mR and the QTF. A beam splitter was inserted, which directs a portion of the EC-QCL radiation to a reference channel consisting of 10 cm long reference cell, filled with a 0.5% NO in N_2 and a pyroelectric detector (InfraTec, LIE-332f-63). The beam splitter allowed most of the laser radiation to pass and provides convenient monitoring of the EC-QCL output with a power meter (Ophir, 3A-SH). The QTF was connected to an ultra-low noise transimpedance amplifier with a 10 MΩ feedback resistor that converted the current generated by QTF into a voltage. This voltage was directed to a custom made control electronics unit (CEU) [14],

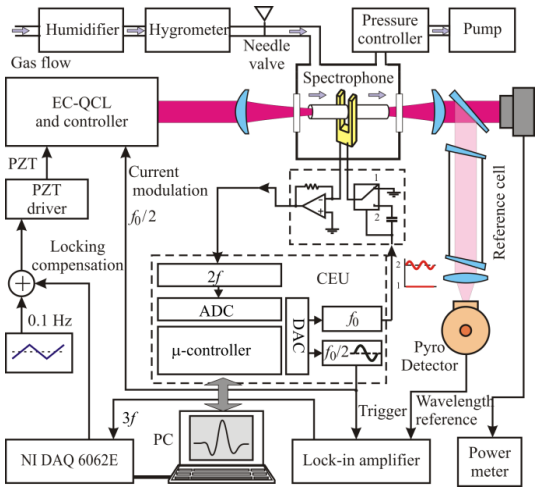

Fig. 2. Schematic of an EC-QCL based NO sensor system.

which was employed to realize three functions: 1. to measure three QTF parameters, i.e. the resonant frequency f_0, quality factor Q and resistance R of the QTF, 2. to modulate the laser current at the frequency $f = f_0/2$, and 3. to measure the $2f$ harmonic component generated by the QTF. The CEU converted the measured current to QEPAS signal counts (1 cnt = 6.67×10^{-16}A). A notebook PC computer communicating with the CEU via a RS232 serial port collected the $2f$ harmonic data. The QTF and mR were enclosed inside a gas enclosure with AR coated ZnSe windows. A pressure controller (MKS Instruments, Inc.,Type 640) and an oil free vacuum pump were placed downstream to control and maintain the NO sensor system pressure. A Nafion humidifier (PermaPure) and a hygrometer (DewMaster, EdgeTech) were connected to the upstream side of the ADM gas cell to add water vapor to the gas mixture and monitor the water content, respectively. A needle valve was employed to set the gas flow to a constant rate of 100 scc/min.

The QEPAS based NO concentration measurements were carried out in two operational modes. In a scan mode a 0.1 Hz triangular wave with amplitude of 25.5 V_{pp} was applied to the piezoelectric translator of the EC-QCL resulting in mode-hop-free QCL frequency tuning over the targeted absorption line. In a locked mode the QCL frequency was initially set to the center of the absorption line. The $3f$ component from the pyroelectric detector was measured by a lock-in amplifier (Stanford Research systems, SR830), subsequently regulated by a Labview-software based proportional-integral-derivative (PID) controller, and finally directed to an electronic adder. The PID controller compensates any laser frequency shift by generating a correction signal to keep the laser frequency always at the center of the absorption line. The electronic adder combined the PID compensation signal and the DC voltage setting the QCL frequency to the center of absorption line, and then directed feed-back to the PZT of the EC-QCL.

#153576 - $15.00 USD Received 7 Sep 2011; revised 22 Oct 2011; accepted 27 Oct 2011; published 10 Nov 2011

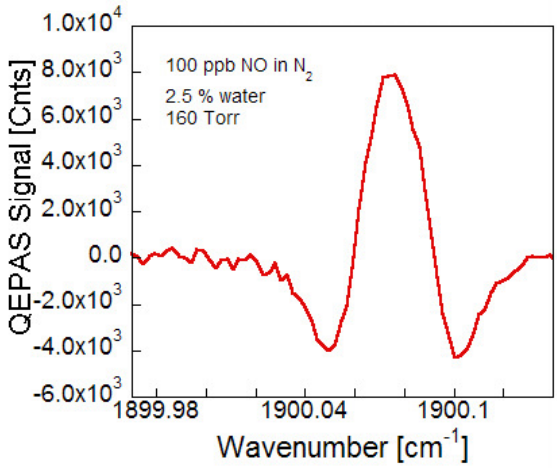

Fig. 3. QEPAS spectra of the NO absorption doublet at 1900.08 cm^{-1}. The QEPAS signal is recorded in terms of internal CEU units, where 1cnt = 6.67×10^{-16}A.

The H_2O and CO_2 interference-free NO doublet absorption lines centered at 1900.08 cm^{-1} were found to be optimal for QEPAS based NO detection [11]. A spectral scan of a 100 ppb NO sample at 160 Torr is depicted in Fig. 3. In this scan, there was no background subtraction performed. Compared to Ref [9], no fringe-like interference pattern was observed in Fig. 3, which is the result of using mR tubes with optimal dimensions. The two lines in the doublet are so close that they are unresolved even at low pressure conditions. To optimize NO

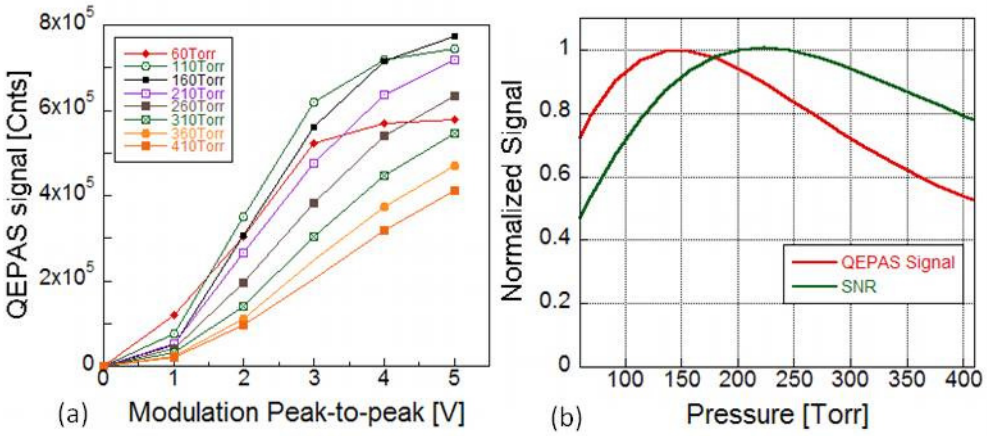

Fig. 4. (a) QEPAS signal corresponding to the peak NO absorption at 1900.08 cm^{-1} for 8 different gas pressures as a function of laser current modulation depth. All measurements were carried out with a 10-ppmv NO in a N_2 mixture containing a 2.5% water concentration; (b) normalized QEPAS signal and SNR as a function of gas mixture pressure.

QEPAS detection performance, both the gas pressure and the wavelength modulation depth must be appropriately chosen. In Fig. 4(a), the QEPAS signal corresponding to the peak absorption was mapped as a function of gas pressure and laser current modulation depth. The measurements were carried out with a 10 ppmv NO in N_2 mixture. A 2.5% water concentration was added to the mixture to promote the V-T relaxation rate of NO. Due to the limitation of current modulation input voltage of 0-5 V_{pp}, the modulation depth cannot reach the optimal value when the gas pressures exceeded 160 Torr. The signal amplitude and SNR were plotted in Fig. 4(b) as a function of pressure based on Fig. 4(a) and Eq. (1). It is evident

#153576 - $15.00 USD Received 7 Sep 2011; revised 22 Oct 2011; accepted 27 Oct 2011; published 10 Nov 2011

that the highest signal amplitude is observed at 150 Torr, while the highest SNR is observed at 210 Torr. Therefore, a 210 Torr pressure was selected and used as the optimum pressure value in the section 4 reported experiments.

4. NO relaxation in a H_2O/N_2 mixture

The QEPAS signal amplitude, as already mentioned in section 2, is strongly dependent on the V-T relaxation rate of the target gas. For NO in dry N_2, this rate is slow and equal to τ ~300 μs [15, 16]. For comparison, the V-T energy transfer time for H_2O, which is known as an extremely fast relaxation molecule, is 0.037 μs [12]. The commercial QTFs used in QEPAS so far are available only at a resonant frequency f_0 of ~32.8 kHz, i.e. $1/\omega = 1/2\pi f_0 \approx 5$ μs. This $1/\omega$ value in QEPAS experiments is at least 8 times lower than in conventional PAS experiments where the modulation frequency does not exceed 4 kHz. In the case of a slow V-T relaxation rate with respect to the modulation frequency ($\tau >> 1/\omega$), the translational gas temperature cannot follow fast changes of the laser induced molecular excitation rate, so that the QEPAS signal is weaker than in the case of an instantaneous V-T energy transfer and is given

$$S = S_0 \frac{1}{\sqrt{1+\tan^2\theta}}, \quad \tan\theta = \omega\tau(C_{tr}/C_0), \tag{3}$$

where S_0 is the signal for instantaneous V-T energy transfer, θ is the phase shift between the excitation and QEPAS signal, C_{tr} and C_0 are the translational-rotational heat capacity and total heat capacity at constant volume, respectively [12].

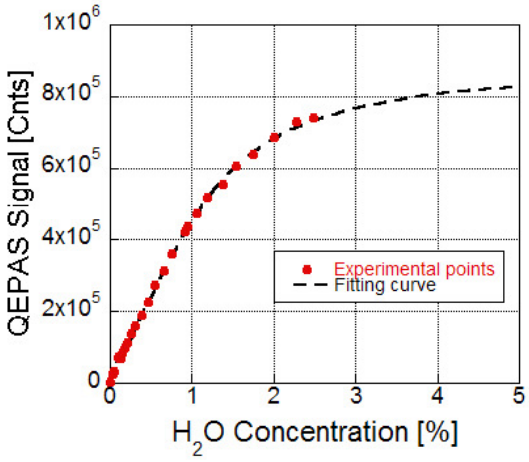

Fig. 5. QEPAS signal of NO as a function of added water concentration. Total gas pressure is 210 Torr . 1cnt = 6.67×10^{-16}A

With a 10 ppm dry NO in N_2 mixture, the QEPAS signal is only ~5900 counts. Direct V-T energy transfer from vibrationally excited NO in a NO/N_2 mixture can be excluded from consideration on a $1/\omega$ time scale due to a slow NO V-T transfer time. The observed NO QEPAS signal in dry NO/N_2 mixture at 32.8 kHz is mostly the result of rotational relaxation that has the faster relaxation process. Moreover, at low pressures the mean diffusion path of the excited molecule is comparable with the mR radius. The diffusion of the initially exited NO molecules to the mR tube wall with the subsequent V-T relaxation on the wall also contributes to the QEPAS signal level [5, 17].

A significant enhancement of the NO QEPAS signal amplitude can be achieved by blending an analyzed mixture with water vapor, which is known to be an efficient catalyst for

#153576 - $15.00 USD Received 7 Sep 2011; revised 22 Oct 2011; accepted 27 Oct 2011; published 10 Nov 2011

the vibrational energy transfer reactions in the gas phase. This effect of water vapor on the level of NO QEPAS signal is especially helpful in environmental and exhaled human breath measurements, for which the typical amount of water vapor in ambient air and human breath is 1-4% and ~5%, respectively. Therefore, a detailed analysis of the effect of H_2O on NO QEPAS signal is essential for precise NO concentration measurements.

To analyze the influence of H_2O on NO relaxation, a certified mixture of 10 ppm NO in N_2 was used. The amplitude of 2*f* QEPAS signal was measured in the locked mode at 210 Torr pressure and for different water concentrations. The results are shown in Fig. 5. A 0.5% addition of water resulted in a 43 times signal enhancement. For a 2.5% water vapor concentration, a 130 times enhancement factor was achieved. Due to instrumental limitations of the humidifier, a condition of 5% water vapor concentration, which is similar to the concentration in exhaled human breath, could not be simulated. However, according to the fitting curve [5], the estimated enhancement factor can reach 146 times in the case of a 5% water vapor concentration.

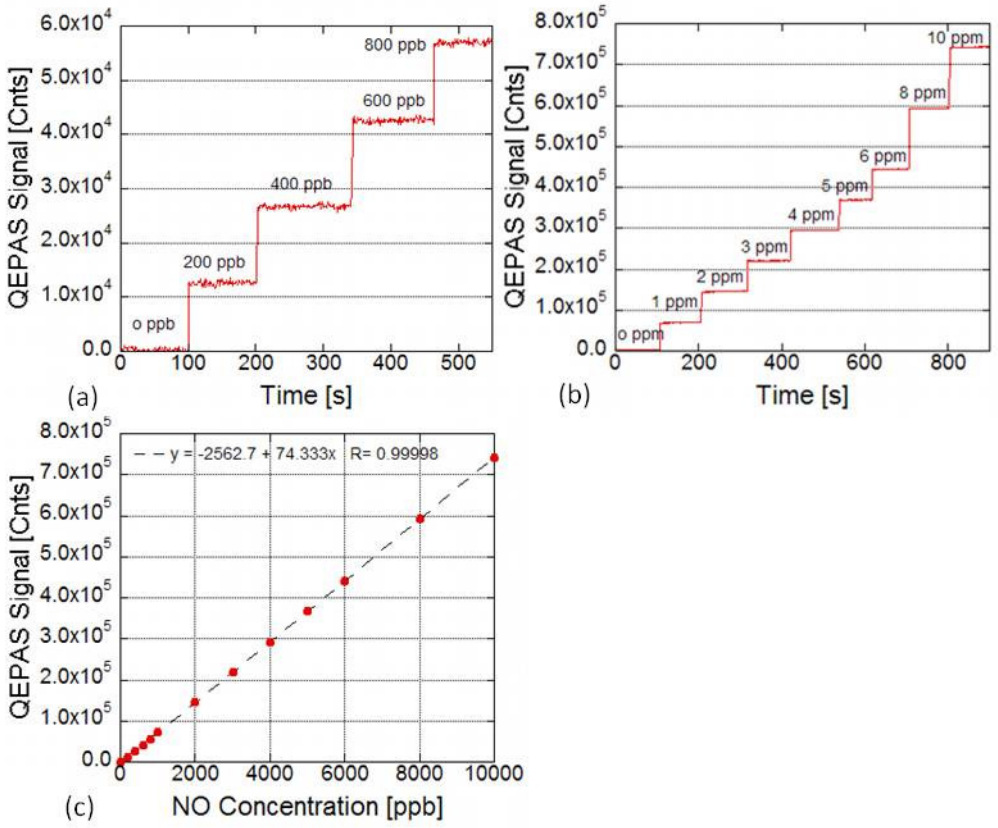

Fig. 6. (a) (b) QEPAS signal is repetitively recorded in locked mode as the NO concentration is varied. (c) Same data averaged and plotted as a function of the NO concentration based on the calibration of the gas dilution system. 1cnt = 6.67×10^{-16}A

5. Performance assessment of NO QEPAS sensor

To evaluate the performance of the EC-QCL based QEPAS platform for NO detection described in section 3, the system was operated in the locked mode. The NO concentration measurements were carried out at 210 Torr pressure and with maximum current modulation achieved by applying a 5 V_{pp} sine wave to the current modulation input of the EC-QCL controller. A constant water concentration of 2.5% was added to the NO/N_2 mixture using the

#153576 - $15.00 USD Received 7 Sep 2011; revised 22 Oct 2011; accepted 27 Oct 2011; published 10 Nov 2011

humidifier. A commercial gas dilution system (Environics, series 4040) and a certified mixture of 10 ppm NO in N_2 were used to produce the various NO concentrations levels. The NO dilution results acquired with a 1-s averaging time (0.785 Hz bandwidth) and 66 mW EC-QCL excitation power are plotted in Fig. 6(a) and Fig. 6(b). The phase of the detected signal was found to be independent of the NO concentration. The scatter of consecutive measurements at certain concentration levels also did not depend on the concentration and was in agreement with Eq. (1). Based on the data in Fig. 6(a) and (b), the NO concentration that results in a noise-equivalent (1σ) concentration with a 1s averaging time is 4.9 ppbv. The corresponding absorption coefficient normalized to the detection bandwidth and optical power is 5.6×10^{-9} $cm^{-1}W/Hz^{1/2}$. This minimum detection limit for NO is achieved as the result of the optimal mR design and the faster V-T relaxation rate induced by the presence of 2.5% water vapor. This result is only slightly higher than the value 3.3×10^{-9} $cm^{-1}W/Hz^{1/2}$ measured for C_2H_2 detection using the NIR optimal mR tube size [6].

In order to verify the linearity for NO concentration measurement, all the readings of each concentration step are averaged and plotted in Fig. 6(c). This plot confirms the linearity of the system response to concentration. The dynamic range of the NO QEPAS sensor covers at least four orders of magnitude.

6. Conclusions

In summary, it was demonstrated that the QEPAS sensor design based on two acoustic mR tubes with wider internal diameters and shorter lengths as compared to optimum design for NIR lasers is optimal for MIR trace-gas detection using QCLs. Unlike the previous mR performance of a MIR QEPAS gas sensor reported in Ref [9], the 3.9 mm long mR tubes with an internal diameter of 0.84 mm eliminate the interference pattern superimposed on the QEPAS signal, resulting in a background-free thermal-noise-limited QEPAS 2*f* signal. Thus, background subtraction based on the averaging of spectral multi-scans can be avoided. Instead, the laser wavelength can be locked to the target absorption line center to monitor the trace gas concentration, which facilitates data processing as well improves the detection sensitivity. The NO detection limit of 4.9 ppbv with 1-s averaging time achieved so far is ~10 times better than the result reported in Ref [9] if the same laser power and averaging time are employed. The present minimum detection limit can be further improved if higher power CW, single frequency QCL devices become available or if the sensor application permits the use of longer signal averaging times. Furthermore, the use of CW distributed feedback (DFB) QCL sources will allow larger wavelength modulation ranges as compared to an EC-QCL, which can be beneficial at operating pressure of >160 Torr in the ADM. The presence of water vapor in the analyzed mixture can efficiently promote the NO V-T relaxation rate resulting in a stronger QEPAS signal. However, different water vapor concentrations lead to different sensitivities. Hence it is necessary to control and monitor the water concentration that is present in a NO QEPAS based sensor. The QEPAS sensor architecture when compared to other laser spectroscopic techniques potentially allows the conversion of a laboratory setup into a compact, portable device suitable for applications in environmental monitoring and medical diagnostics of human diseases based on exhaled breath analysis as well as in industrial processing.

Acknowledgments

The Rice University group acknowledges financial support from a National Science Foundation ERC MIRTHE award and a grant C-0586 from the Welch Foundation. V. Spagnolo acknowledges financial support from the Regione Puglia “Intervento Cod. DM01, Progetti di ricerca industriale connessi con la strategia realizzativa elaborata dal Distretto Tecnologico della Meccatronica”.

#153576 - $15.00 USD Received 7 Sep 2011; revised 22 Oct 2011; accepted 27 Oct 2011; published 10 Nov 2011